2019

Pharmacological blockade of the CD39/CD73 pathway but not adenosine receptors augments disease in a humanized mouse model of graft-versus-host disease

Nicholas Geraghty
University of Wollongong, ng646@uowmail.edu.au

Debbie Watson
University of Wollongong, dwatson@uow.edu.au

Ronald Sluyter
University of Wollongong, rsluyter@uow.edu.au

Publication Details

Geraghty, N. J., Watson, D. & Sluyter, R. (2019). Pharmacological blockade of the CD39/CD73 pathway but not adenosine receptors augments disease in a humanized mouse model of graft-versus-host disease. Immunology and Cell Biology, 97 (6), 597-610.

Pharmacological blockade of the CD39/CD73 pathway but not adenosine receptors augments disease in a humanized mouse model of graft-versus-host disease

Abstract

Allogeneic hematopoietic stem cell transplantation is a curative therapy for a number of hematological malignancies, but is limited by the development of graft-versus-host disease (GVHD). CD39 and CD73 form an ectoenzymatic pathway that hydrolyzes extracellular adenosine 5′-triphosphate (ATP) to adenosine, which respectively exacerbate or alleviate disease in allogeneic mouse models of GVHD. The current study aimed to explore the role of the CD39/CD73 pathway and adenosine receptor (AR) blockade in a humanized mouse model of GVHD. Immunodeficient nonobese diabetic-severe combined immunodeficiency-IL-2 receptor γ^{null} mice were injected with human peripheral blood mononuclear cells, and subsequently injected with the CD39/CD73 antagonist αβ-methylene-ADP (APCP) (50 mg kg^{-1}) or saline for 7 days, or the AR antagonist caffeine (10 mg kg^{-1}) or saline for 14 days. Mice predominantly engrafted human $CD4^+$ and $CD8^+$ T cells, with smaller proportions of human regulatory T cells, invariant natural killer T cells, monocytes and dendritic cells. Neither APCP nor caffeine altered engraftment of these human leukocyte subsets. APCP (CD39/CD73 blockade) augmented GVHD as shown through increased weight loss and worsened liver histology, including increased leukocyte and human T-cell infiltration, and increased apoptosis. This treatment also increased serum human IL-2 concentrations and decreased the frequency of human $CD39^-$ $CD73^-$ $CD4^+$ T cells. In contrast, caffeine (AR blockade) did not alter GVHD severity or human serum cytokine concentrations (IL-2, IL-6, IL-10 or tumor necrosis factor-α). In conclusion, blockade of CD39/CD73 but not ARs augments disease in a humanized mouse model of GVHD. These results indicate that CD39/CD73 blockade maintains sufficient extracellular ATP concentrations to promote GVHD in this model.

Disciplines

Medicine and Health Sciences

Publication Details

Geraghty, N. J., Watson, D. & Sluyter, R. (2019). Pharmacological blockade of the CD39/CD73 pathway but not adenosine receptors augments disease in a humanized mouse model of graft-versus-host disease. Immunology and Cell Biology, 97 (6), 597-610.

Pharmacological blockade of the CD39/CD73 pathway but not adenosine receptors augments disease in a humanised mouse model of graft-versus-host disease

RUNNING TITLE: CD39/CD73 but not adenosine receptor blockade augments graft-versus-host disease

NJ Geraghty[1,2,3], D Watson[1,2,3] and R Sluyter[1,2,3]

[1]School of Chemistry and Molecular Bioscience, University of Wollongong, Wollongong, NSW, 2252, Australia, [2]Molecular Horizons, University of Wollongong, NSW, 2252, Australia, [3]Illawarra Health and Medical Research Institute, Wollongong, NSW, 2252, Australia

Correspondence to: Ronald Sluyter, Associate Professor, School of Chemistry and Molecular Bioscience, University of Wollongong, Illawarra Health and Medical Research Institute, Northfields Avenue, Wollongong, NSW 2522, Australia

Phone: +61 2 4221 5508, email: rsluyter@uow.edu.au

KEY WORDS: Graft-versus-host disease, adenosine receptor, purinergic receptor, CD73, CD39, T lymphocyte, regulatory T cells, invariant natural killer T cells, xenogeneic mice.

ABSTRACT

Allogeneic haematopoietic stem cell transplantation (HSCT) is a curative therapy for a number of haematological malignancies, but is limited by the development of graft-versus-host disease (GVHD). CD39 and CD73 form an ecto-enzymatic pathway that hydrolyses extracellular adenosine 5'-triphosphate (ATP) to adenosine, which respectively exacerbate or alleviate disease in allogeneic mouse models of GVHD. The current study aimed to explore the role of the CD39/CD73 pathway and adenosine receptor (AR) blockade in a humanised mouse model of GVHD. Immunodeficient non-obese diabetic-severe combined immunodeficiency-IL-2 receptor γ^{null} (NSG) mice were injected with human peripheral blood mononuclear cells (PBMCs), and subsequently injected with the CD39/CD73 antagonist αβ-methylene-ADP (APCP) (50 mg/kg) or saline for 7 days, or the AR antagonist caffeine (10 mg/kg) or saline for 14 days. Mice predominantly engrafted human $CD4^+$ and $CD8^+$ T cells, with smaller proportions of human regulatory T (Treg) cells, invariant natural killer T (iNKT) cells, monocytes and dendritic cells (DCs). Neither APCP or caffeine altered engraftment of these human leukocyte subsets. APCP (CD39/CD73 blockade) augmented GVHD as shown through increased weight loss and worsened liver histology, including increased leukocyte and human T cell infiltration, and increased apoptosis. This treatment also increased serum human IL-2 concentrations and decreased the frequency of human $CD39^-CD73^-CD4^+$ T cells. In contrast, caffeine (AR blockade) did not alter GVHD severity or human serum cytokine concentrations (IL-2, IL-6, IL-10 or TNFα). In conclusion, blockade of CD39/CD73 but not ARs augments disease in a humanised mouse model of GVHD. These results indicate that CD39/CD73 blockade maintains sufficient extracellular ATP concentrations to promote GVHD in this model.

INTRODUCTION

Allogeneic haematopoietic stem cell transplantation (HSCT) is a common curative therapy for numerous haematological malignancies. However, 30-60% of transplant recipients develop graft-versus-host disease (GVHD) as a result of the donor T cells recognising the recipient tissue as 'foreign'[1]. The first stage of GVHD is characterised by the initial release of cytokines, such as TNF-α and IL-6, from damaged tissue caused by the underlying disease or pre-conditioning regimes. Following this, activation of $CD4^+$ T cells by antigen presenting cells, such as dendritic cells (DC), can cause release of T helper-1 (Th1) cytokines such as TNF-α, IFN-γ and IL-2. Finally, both $CD4^+$ and $CD8^+$ T cells migrate to the liver, gastrointestinal tract and skin to cause inflammatory damage of these tissues[2]. Alternatively, IL-10 can suppress immune responses and can potentially reduce GVHD[3]. The T cell subsets regulatory T (Treg) cells and invariant natural killer T (iNKT) cells can also reduce GVHD severity[4].

Purinergic signalling includes the plasma membrane P1 and P2 receptors. P1 or adenosine receptors (AR; A_1, A_{2A}, A_{2B} and A_3) are activated by extracellular adenosine, while P2 receptors (P2X1-7 and $P2Y_{1, 2, 4, 6, 8, 11\text{-}14}$) are activated by a range of extracellular nucleotides including adenosine 5'-triphosphate (ATP)[5]. Purinergic receptors are important in inflammation and immunity, and are expressed on immune cells including antigen presenting cells and T cells[6]. In general activation of P2 receptors by extracellular ATP exerts pro-inflammatory effects[7] including T cell activation and migration[8,9]. In contrast, hydrolysis of ATP to adenosine by a pathway involving ecto-nucleoside triphosphate diphosphohydrolase-1 (CD39) and ecto-5'-nucleotidase (CD73) commonly results in anti-inflammatory effects via activation of ARs[10].

ATP, released from activated, damaged or dying cells, can activate P2 receptors and promote inflammatory responses in transplantation[11]. Moreover, P2 receptor activation can promote development of GVHD. Extracellular ATP can be released from damaged cells in GVHD[12] and subsequently activate P2X7 to promote disease development in allogeneic[12-14] and humanised[15,16] mouse models of GVHD. Likewise, P2Y2 activation by ATP can promote leukocyte infiltration and tissue damage in allogeneic models of GVHD[17]. In contrast, activation of ARs can limit GVHD development[18,19]. Moreover, pharmacological blockade of ARs with caffeine[20] or A_{2A} with SCH58261[21] or genetic deletion of A_{2A}[20,21] worsens disease in allogeneic mouse models of GVHD. Similarly, pharmacological blockade of CD39 and CD73 with αβ-methylene-ADP (APCP), which prevents adenosine generation and increases extracellular ATP[22,23], augments GVHD in allogeneic mouse models[21]. However, the roles of the CD39/CD73 pathway and ARs in a humanised mouse model of GVHD have not been reported.

Using pharmacological approaches, the current study aimed to investigate the role of the CD39/CD73 pathway and AR blockade in disease development in a humanised mouse model of GVHD. In this model, immunodeficient non-obese diabetic-severe combined immunodeficiency-IL-2 receptor γ^{null} (NSG) mice are injected with human peripheral blood mononuclear cells (PBMC) and develop clinical signs of GVHD over 10 weeks[15]. CD39/CD73 blockade with APCP, but not AR blockade with caffeine, augments GVHD in humanised mice. These results support the known roles of extracellular ATP in promoting GVHD, but do not provide evidence that extracellular adenosine can limit GVHD in this humanised model.

RESULTS

APCP does not impact hPBMC engraftment in NSG mice

To investigate a role for the CD39/CD73 pathway in GVHD development in humanised NSG mice, these mice were injected with the CD39/CD73 inhibitor, APCP, using the same regime efficacious in an allogneic mouse model of GVHD[20]. First, to investigate whether APCP (CD39/CD73 blockade) altered hPBMC engraftment in NSG mice, 3 weeks post-hPBMC injection blood cells from APCP- (n = 9) or saline-injected (n = 9) mice were analysed by flow cytometry. APCP- and saline-injected mice demonstrated similar frequencies of human leukocytes ($hCD45^+mCD45^-$ cells), calculated as a percentage of total leukocytes ($hCD45^+mCD45^-$/($hCD45^+mCD45^-$ and $hCD45^-mCD45^+$) (22.1 ± 3.9% and 22.2 ± 5.4%, respectively, $P = 0.9869$) (Fig 1a). These human leukocytes from APCP- and saline-injected mice predominately comprised T cells ($hCD3^+hCD19^-$) (99.5 ± 0.1% and 99.3 ± 0.3%, respectively, $P = 0.4897$) (Fig 1b), with a small amount of non-B/T cells ($hCD3^-$ $hCD19^-$) (0.5 ± 0.1% and 0.7 ± 0.3%, respectively, $P = 0.4897$) (Fig 1c).

At end-point, splenocytes from APCP- ($n = 9$) and saline-injected ($n = 8$) mice were analysed by flow cytometry. APCP- and saline-injected mice demonstrated similar frequencies of human leukocytes (75.1 ± 9.4% and 90.2 ± 3.0%, respectively, $P = 0.1691$) (Fig 1d). One APCP-injected mouse revealed a human leukocyte frequency of only 9.7% (Fig 1d) but was included in subsequent analyses. APCP- and saline-injected mice demonstrated similar frequencies of human T cells (92.5 ± 1.9% and 95.1 ± 1.6%, respectively, $P = 0.3128$) (Fig 1e), which comprised both $hCD4^+$ T cells (58.3 ± 6.5% and 64.0 ± 7.0%, respectively, $P = 0.5558$) and $hCD8^+$ T cells (29.6 ± 6.0% and 19.2 ± 3.3%, respectively, $P = 0.1633$) (Fig 1f). Both APCP- and saline-injected mice demonstrated greater frequencies of $hCD4^+$ T cells than $hCD8^+$ T cells ($P = 0.0053$ and $P < 0.0001$, respectively) (Fig 1f).

To investigate whether APCP altered the frequency of $CD39^{+/-}$ and/or $CD73^{+/-}$ human T cells, these markers on $hCD4^+$ and $hCD8^+$ T cells from the spleens of humanised mice were analysed by flow cytometry. APCP-injected mice, compared to saline-injected mice, demonstrated a trend of increased $hCD39^+hCD73^-hCD4^+$ T cells and $hCD39^-hCD73^+hCD4^+$ T cells, but a similar frequency of $hCD39^+hCD73^+hCD4^+$ T cells (Fig 1g; Table 2). Conversely, the frequency of $hCD39^-hCD73^-hCD4^+$ T cells was significantly reduced in APCP-injected mice compared to saline-injected mice (Table 2). In contrast to $hCD4^+$ T cells, APCP- and saline-injected mice demonstrated similar frequencies of these respective $hCD8^+$ T cell subsets (Fig 1h; Table 2).

Previous studies have demonstrated that increased proportions of iNKT and Treg cells correlate to reduced GVHD severity in allogeneic mouse models of GVHD[4], but the presence of human iNKT cells in humanised NSG mice is unknown. Therefore, the presence and frequency of human iNKT cells ($hCD45^+hCD3^+hCD19^-hV\alpha24\text{-}J\alpha18^+$), as well as human Treg cells ($hCD45^+hCD3^+hCD4^+hCD25^+hCD127^{lo}$), in the spleens of these mice was examined. APCP- and saline-injected mice demonstrated the presence and similar frequencies of iNKT cells (2.4 ± 1.0% and 1.4 ± 0.4%, respectively, $P = 0.3674$) (Fig 1i). APCP- and saline-injected mice also demonstrated similar frequencies of Treg cells (1.4 ± 0.6 and 0.9 ± 0.2%, respectively, $P = 0.4983$) (Fig 1j).

Previously, our group observed that the spleens of humanised mice at end-point do not contain human B cells[15]. Consistent with this observation, the remaining human leukocytes in the spleens of APCP- and saline-injected mice were negative for CD19, with similar frequencies of $CD3^-CD19^-$ cells present in both groups of mice (7.5 ± 1.9% and 3.2 ± 1.0%, respectively, $P = 0.0703$) (Fig 1k). Therefore, this remaining non-B/T cell population ($hCD45^+hCD3^-hCD19^-$) was further analysed to determine if these cells were human monocytes ($hCD14^+hCD83^-$) or DCs ($hCD14^-hCD83^+$). APCP- and saline-injected mice

demonstrated small but similar frequencies of human monocytes (0.03 ± 0.02% and 0.001 ± 0.001%, respectively, $P = 0.1804$) (Fig 1l) and human DCs (0.4 ± 0.2% and 0.3 ± 0.1%, respectively, $P = 0.6066$) (Fig 1m).

APCP augments clinical and histological GVHD in humanised mice

To investigate whether APCP (CD39/CD73 blockade) impacted GVHD development, the above mice were monitored for disease development for up to 10 weeks. APCP-injected mice ($n = 9$) demonstrated significantly greater weight loss over the 10 weeks than saline-injected mice ($n = 9$) ($P = 0.0350$) (Fig 2a). APCP-mice demonstrated signs of GVHD (classified as a clinical score ≥ 3)[24] from 38 days onwards, while saline-injected mice demonstrated signs of GVHD from 45 days, however, clinical scores were similar over 10 weeks ($P = 0.1711$) (Fig 2b). Moreover, APCP- and saline-injected mice exhibited identical median survival times (MST) (57 days and 57 days, respectively, $P = 0.2634$) and similar mortality over 10 weeks (100% and 78%, respectively, $P = 0.2059$) (Fig 2c).

GVHD affects the liver, gastrointestinal tract and skin in humans[25], and in allogeneic[26] and humanised[27] mouse models. APCP-injected mice exhibited greater histological damage and leukocyte infiltration into the liver (1052.0 ± 110.0 cells field of view^{-1}, $n = 9$) compared to saline-injected mice (727.8 ± 98.0 cells field of view^{-1}, $n = 9$) ($P = 0.0216$) (Fig 3a-b). In contrast, the small intestines of APCP- and saline-injected mice exhibited similar amounts of leukocyte infiltration (234.7 ± 46.6 cells field of view^{-1}, $n = 9$ and 196.4 ± 34.1 cells field of view^{-1}, $n = 9$, respectively, $P = 0.5179$), crypt epithelial cell apoptosis and structural damage including rounding of villi (Fig 3a-b). Similarly, the skin of APCP- and saline-injected mice displayed similar amounts of leukocyte infiltration (512.8 ± 64.5 cells field of view^{-1}, $n = 9$ and 617.8 ± 78.1 cells field of view^{-1}, $n = 9$, respectively, $P = 0.3127$), with similar but minimal amounts of basal epithelial cell apoptosis and epidermal thickening (Fig 3a-b).

Livers from APCP-injected mice demonstrated significantly increased human T cell infiltration (62.0 ± 12.1 cells field of view^{-1}, n = 4) compared to saline-injected mice (31.4 ± 4.4 cells field of view^{-1}, n = 4) (P = 0.0271) (Fig 3c-d). Livers from APCP-injected mice also demonstrated increased apoptotic cells (270 ± 62.5 cells field of view^{-1}, n = 4) compared to saline-injected mice (126.1 ± 10.7 cells field of view^{-1}, n = 4) (P = 0.0319) (Fig 3e-f). Similar to histological observations, APCP- and saline-injeccted mice demonstrated similar numbers of apoptotic cells in the small intestines (43.8 ± 15.1 cells field of view^{-1}, n = 3 and 42.2 ± 15.5 cells field of view^{-1}, n = 3, P = 0.9450) and skin (40.4 ± 11.3 cells field of view^{-1}, n = 4 and 25.8 ± 3.1 cells field of view^{-1}, n = 4, P = 0.2576) (Fig 3e-f).

APCP blockade increases serum hIL-2 concentrations in humanised mice

An important part of GVHD development is the pro-inflammatory cytokine storm that drives immune cell proliferation and inflammatory damage[2]. Therefore, to determine if APCP altered cytokine production in humanised mice, serum hIL-2, hIL-6, hIL-10, hTNF-α and hIFN-γ concentrations from APCP- (n = 9) and saline-injected (n = 8) mice were analysed by a flow cytometric multiplex assay. APCP-injected mice demonstrated a significant increase in serum hIL-2 concentrations (3.2 ± 0.5 pg mL^{-1}) compared to saline-injected mice (1.6 ± 0.3 pg mL^{-1}) (P = 0.0080) (Fig 4a). In contrast, APCP- and saline-injected mice demonstrated similar serum concentrations of hIL-6 (3.9 ± 1.5 pg mL^{-1}, and 1.4 ± 0.7 pg mL^{-1}, respectively, P = 0.1743) (Fig 4b), hIL-10 (22.2 ± 4.1 pg mL^{-1}, and 19.1 ± 3.1 pg mL^{-1}, respectively, P = 0.7621) (Fig 4c), and TNF-α (21.3 ± 6.5 pg mL^{-1}, and 16.6 ± 3.4 pg mL^{-1}, respectively, P = 0.7851) (Fig 4d). Serum hIFN-γ concentrations in both treatment groups exceeded the highest standard (>10,000 pg mL^{-1}) and thus could not be compared (data not shown). Attempts to reassess serum hIFN-γ concentrations by ELISA were unsuccessful (results not shown), possibly due to freeze-thawing of serum.

To determine if APCP impacted hA_{2A} or hP2X7 expression, mRNA expression of these molecules in the spleen was measured by qPCR. APCP- and saline-injected mice demonstrated similar relative mRNA expression of hA_{2A} (0.22 ± 0.09 and 0.10 ± 0.03, respectively, P = 0.2863) (Fig 4e) and hP2X7 (1.0 ± 0.3 and 0.9 ± 0.3, respectively, P = 0.8984) (Fig 4f).

To confirm APCP does not impact P2X7 an ATP-induced YO-PRO-1^{2+} uptake assay was performed. Freshly isolated hPBMCs were preincubated in the absence or presence of APCP or the P2X7 antagonist Brilliant Blue G (BBG), and ATP-induced YO-PRO-1^{2+} uptake was assessed. ATP induced significant YO-PRO-1^{2+} uptake into $hCD3^+$ T cells, which was not affected by preincubation with APCP, but reduced by 99% by preincubation with BBG (P < 0.005, n = 3) (Fig 4g). There was no significant difference in YO-PRO-1^{2+} uptake between treatments in the absence of ATP (data not shown).

Caffeine does not impact hPBMC engraftment in NSG mice

The above data suggests that decreased adenosine and/or increased ATP production due to APCP-mediated blockade of CD39/CD73 worsens GVHD in humanised NSG mice. Thus, a role for ARs using the broad-spectrum AR antagonist, caffeine, in this process was examined using the same regime efficacious in an allogeneic mouse model of GVHD[20]. First, to determine if caffeine altered hPBMC engraftment, 3 weeks post-hPBMC injection blood cells from caffeine- (n = 13) and saline-injected (n = 15) mice were analysed by flow cytometry. Caffeine- and saline-injected mice demonstrated similar frequencies of human leukocytes (23.5 ± 3.5% and 28.5 ± 4.7%, respectively, P = 0.4135) (Fig 3a), which comprised T cells (92.5 ± 1.1% and 94.2 ± 0.7%, respectively, P = 0.1897) (Fig 3b), and non-B/T cells (7.5 ± 1.1% and 5.8 ± 0.7%, respectively, P = 0.1897) (Fig 3c).

At end-point, splenocytes from caffeine- (n = 13) and saline-injected (n = 14) mice were analysed by flow cytometry. Caffeine- and saline-injected mice demonstrated similar frequencies of human leukocytes (72.2 ± 6.2% and 75.6 ± 3.8%, respectively, P = 0.6346) (Fig 3d). One caffeine-injected mouse revealed a human leukocyte frequency of only 11.2% (Fig 3d) but was included in subsequent analyses. Caffeine- and saline-injected mice demonstrated similar frequencies of human T cells (96.1 ± 1.0% and 93.7 ± 1.9%, respectively, P = 0.2934) (Fig 3e), which comprised $hCD4^+$ T cells (51.7 ± 4.4% and 52.7 ± 3.4%, respectively, P = 0.8658) and $hCD8^+$ T cells (13.5 ± 2.3% and 18.5 ± 4.0%, respectively, P = 0.3011). Both caffeine- and saline-injected mice demonstrated greater frequencies of $hCD4^+$ than $hCD8^+$ T cells ($P < 0.0001$ and $P < 0.0001$, respectively) (Fig 3f). Caffeine- and saline injected mice demonstrated similar frequencies of $CD4^+$ and $CD8^+$ T cell subsets expressing CD39 and/or CD73 or neither of these molecules (Fig 3g, h; Table 3).

Caffeine- and saline-injected mice also demonstrated similar frequencies of iNKT cells (3.1 ± 0.9% and 1.6 ± 0.3%, respectively, P = 0.1088) (Fig 3i) and Treg cells (0.8 ± 0.1% and 0.9 ± 0.2%, respectively, P = 0.8964) (Fig 3j). Caffeine- and saline-injected mice demonstrated similar frequencies of non-B/T cells (4.1 ± 1.1% and 5.8 ± 1.9%, respectively, P = 0.4381) (Fig 3k), which included similar frequencies of monocytes (0.2 ± 0.1%, n = 11 and 0.3 ± 0.1%, n = 10 respectively, P = 0.5873) (Fig 3l) and DCs (0.6 ± 0.2%, n = 11 and 0.4 ± 0.2%, n = 10 respectively, P = 0.7984) (Fig 3m).

Caffeine does not impact clinical or histological GVHD in humanised mice

To determine if caffeine (AR blockade) impacted GVHD development, the above mice were monitored for disease development for up to 10 weeks. Caffeine- (n = 13) and saline-injected (n = 15) mice demonstrated similar weight loss (P = 0.7574) (Fig 4a) and clinical scores (P = 0.0846) (Fig 4b) over 10 weeks. Moreover, caffeine- and saline-injected mice exhibited

similar MSTs (47 days and 45 days, respectively, $P = 0.8741$) and mortality over 10 weeks (87% and 87%, respectively, $P = 1.000$) (Fig 4c).

Caffeine- and saline-injected mice demonstrated similar amounts of leukocyte infiltration and histological damage of the liver, small intestine and skin (Fig 4d). Moreover, the small intestines from mice from either group exhibited similar amounts of structural damage including enterocyte loss, crypt epithelial cell apoptosis and rounding of villi (Fig 2d). Similarly, skin from both caffeine- and saline-injected mice displayed mild basal epithelial cell apoptosis and epidermal thickening (Fig 2d).

Caffeine does not impact serum cytokine concentrations in a humanised mouse model of GVHD

Finally, to determine if caffeine altered cytokine production in humanised mice, serum hIL-2, hIL-6, hIL-10, hIFN-γ and hTNF-α concentrations were analysed as above. Caffeine- (n = 12) and saline-injected (n = 11) mice demonstrated similar concentrations of serum hIL-2 (1.5 ± 0.4 pg mL^{-1} and 1.0 ± 0.3 pg mL^{-1}, respectively, $P = 0.7556$), hIL-6 (2.9 ± 1.3 pg mL^{-1} and 3.7 ± 2.8 pg mL^{-1}, respectively, $P = 0.6577$), and hIL-10 (23.0 ± 2.6 pg mL^{-1} and 26.8 ± 6.4 pg mL^{-1}, respectively, $P = 0.8594$). There was a trend of increased hTNF-α concentration in caffeine-injected mice, which approached but did not achieve statistical significance (18.6 ± 3.2 pg mL^{-1} and 13.7 ± 3.3 pg mL^{-1}, respectively, $P = 0.0852$). Serum hIFN-γ concentrations in both treatment groups exceeded the highest standard (>10,000 pg mL^{-1}) and thus could not be compared (data not shown). Attempts to reassess serum hIFN-γ concentrations by ELISA were unsuccessful (results not shown), possibly due to freeze-thawing of serum.

DISCUSSION

Accumulation of extracellular adenosine resulting from the CD39/CD73 pathway and subsequent activation of ARs is important in limiting disease in allogeneic mouse models of GVHD[20,21]. However, the role of this signalling axis in humanised mouse models of GVHD remained unknown. The current study demonstrated that CD39/CD73 blockade with APCP increases weight loss, liver GVHD and serum hIL-2 concentrations, and decreases the frequency of $hCD39^{-}hCD73^{-}hCD4^{+}$ T cells in humanised mice. In contrast, blockade of ARs with caffeine did not impact clinical or histological GVHD or associated leukocytes or inflammatory markers. It is unlikely that caffeine failed to block ARs in the humanised mice, as this same caffeine regime augmented GVHD in allogeneic mice[20] and caffeine impairs both murine and human ARs with similar efficacy[28,29]. Thus, the results of this study do not support a role for AR activation in limiting GVHD in humanised mice. Rather, this study supports a role for extracellular ATP in augmenting GVHD in this model. Blockade of CD39 and/or CD73 with APCP maintains or increases extracellular ATP concentrations[22,23]. This ATP in turn may subsequently act on P2X7 and/or P2Y2 to promote GVHD in humanised mice. These P2 receptors are involved in GVHD progression in humanised[15,16] and/or allogeneic models[12-14,17] of this disease, although the role of P2Y2 in the former remains to be elucidated. Furthermore, given that APCP did not alter mortality or histological gastrointestinal tract or cutaneous GVHD in humanised mice, the impact of this compound on extracellular ATP concentrations and subsequent P2X7 and/or P2Y2 activation my be limited.

The current study demonstrates that CD39/CD73 blockade with APCP augments liver GVHD, including increased leukocyte infiltration, human T cell infiltration and apoptosis in humanised mice. This finding is similar to the increased liver GVHD in CD73 deficient mice compared to wild-type mice in allogenic GVHD[20,21]. The inability of AR blockade with

caffeine to augment liver GVHD in humanised mice supports the concept that extracellular ATP rather than adenosine contributes to liver GVHD in humanised mice. In support of this, ATP activation of P2X7 worsens liver GVHD in an allogeneic mouse model[12], and pharmacological blockade of P2X7 reduces liver GVHD in both allogeneic[12,14] and humanised[15,16] mouse models of this disease. Moreover, two of these studies [14,16] indicate that the liver may be particularly sensitive to P2X7-mediated damage in both allogeneic and humanised mice.

The current study also demonstrated the presence of serum hIL-2, hIL-6, hIL-10, hTNF-α and hIFN-γ in humanised mice with GVHD, and implicates a pro-inflammatory role for hIL-2 in GVHD development in this model. Presumably this cytokine is acting on donor human effector T cells as host murine leukocytes in NSG mice do not express functional IL-2 receptors due to the absence of the IL-2 receptor γ chain[30] and since either donor human $CD4^+$ or $CD8^+$ T cells are sufficient to mediate GVHD in humanised NSG mice[31-33]. Consistent with this, administration of low dose IL-2 in allogeneic and humanised mouse models of GVHD results in the activation of donor effector T cells[34,35], which circumvent any potential clinical benefits imparted by the expanded Treg cell population in these mice[35]. Notably, co-administration of IL-10 with IL-2 can limit the expansion of effector T cells and increase survival in humanised mice with GVHD[34]. However in the current study, hIL-10 concentrations where similar in APCP- and saline-injected mice suggesting that any potential effects of hIL-10 on hIL-2 was the same between treatments. Finally, in the current study, serum concentrations of hIL-2, hIL-6, hIL-10 and hTNF-α were in the pg mL^{-1} range, which contrasted the 1000-fold greater amounts of serum hIFN-γ. Thus, this suggests hIFN-γ may have a major role in disease development in this humanised mouse model of GVHD. Consistent with this, P2X7 blockade in this model reduced histological GVHD, which coincided with reduced concentrations of serum hIFN-γ[15].

The current study demonstrated that APCP but not caffeine decreases human $CD39^-CD73^-CD4^+$, but not $CD39^-CD73^-CD8^+$ T cells. The reduced frequency of human $CD39^-CD73^-CD4^+$ T cells due to APCP treatment may be due a compensatory mechanism that involves upregulating CD39 and/or CD73 to increase ATP degradation and promote adenosine generation. This is supported by the trend of increased frequencies of human $CD39^+CD73^-CD4^+$ and $CD39^-CD73^+CD4^+$ T cells following APCP treatment. However, these increases were not statistically significant and there was no increased trend in human $CD39^+CD73^+CD4^+$ T cells in these mice. Thus, the reason for the reduced frequency of human $CD39^-CD73^-CD4^+$ T cells following APCP treatment *in vivo* requires further elucidation.

The current study confirms that NSG mice injected with hPBMCS engraft $hCD4^+$ and $hCD8^+$ T cells as well as Tregs, but shows for the first time that humanised NSG mice also engraft human iNKT cells. This engraftment of human iNKT cells suggests that this model could be used to study these cells *in vivo* and allow manipulation of these cell types to alter disease outcomes. In allogeneic mouse models of GVHD, both host[36] and donor[37] iNKT cells can attenuate disease, whilst adoptive transfer of these cells can prevent GVHD in such models[38]. The current study also demonstrates that humanised NSG mice engraft human monocytes and DCs. Previous studies have shown that NSG mice engraft human monocytes and DCs when injected with human cord blood[39], and engraft human monocytes when injected with hPBMCs[40,41]. Similarly, SCID mice injected with hPBMCs engraft human DCs[42], but the current study is the first to demonstrate DC engraftment in NSG mice injected with hPBMCs. Human T cells recognise murine major histocompatibility complex I and II molecules in NSG mice to cause GVHD[27], but the identity of the APCs involved remains to be determined. However it is known that both host and donor APCs are involved in GVHD development in allogeneic mouse models of this disease[43,44]. The engraftment of human monocytes and DCs

in NSG mice suggests that human T cells may at least in part be activated by human antigen presenting cells in this model. A large proprotion of the non-B/T cell population remain unidentified, but may represent NK cells, which can be present in humanised NSG mice[16]. Finally, it should be noted that a limitation of this study was that proportions and not absolute numbers of each subset were determined.

In conclusion, CD39/CD73 blockade with APCP, but not AR blockade with caffeine, augmented GVHD in humanised mice. These results support the known roles of extracellular ATP in promoting GVHD but do not support evidence that extracellular adenosine can limit GVHD in this humanised model. This data provides further support for P2X7 blockade as a therapeutic approach to prevent GVHD in humans, but does not exclude the use of A_{2A} activation as an alternate or additional therapeutic approach to prevent GVHD in humans.

METHODS

Humanised mouse model of GVHD

Experiments involving human blood and mice were approved by the respective Human and Animal Ethics Committees (University of Wollongong, Wollongong, Australia). A humanised mouse model of GVHD was used as described[24] using human blood from two male and one female healthy adult donors. Briefly, hPBMCs, isolated by density centrifugation using Ficoll-Paque PLUS (GE Healthcare; Uppsala, Sweden), were injected intra-peritoneally (i.p.) (10×10^6 hPBMCs mouse^{-1}) into female NSG mice aged 5-7 weeks (Australian BioResources; Moss Vale, Australia). For CD73 blockade, humanised mice were injected i.p. daily with APCP (Sigma-Aldrich; St Louis, MO, USA) (50 mg kg^{-1}) or saline 2 hours following hPBMC injection and then daily over the next 6 days[20]. For AR blockade, mice were injected i.p. daily with caffeine (Sigma-Aldrich) (10 mg kg^{-1}) or saline 2 hours

following hPBMC injection and then daily for the next 13 days[20]. At 3 weeks post-hPBMC injection, mice were checked for engraftment by immunophenotyping of tail vein blood. Mice were monitored for signs of GVHD using a scoring system, giving a total clinical score out of 10 (Table 1), as described[15]. Mice were euthanized at 10 weeks post-injection of hPBMCs, or earlier if exhibiting a clinical score of ≥ 8 or a weight loss of ≥ 10%, according to the approved animal ethics protocol.

Immunophenotyping by flow cytometry

Tail vein blood (week 3) and spleen cells (end-point) were obtained from mice and lysed with ammonium chloride potassium buffer and immunophenotyped as described[15] using the antibodies listed in Table S1 and the gating strategy depicted in the Supplementary Figures S1 and S2. Data was collected using a BD (San Jose, CA, USA) Fortessa-X20 Flow Cytometer (using band pass filters 450/50 for BV421, 710/50 for BV711, 525/50 for FITC, 586/15 for PE, 695/40 for PerCP-Cy5.5, 780/60 for PE-Cy7 and 670/30 for APC). The relative percentages of cells were analyzed using FlowJo software v8.7.1 (TreeStar Inc.; Ashland, OR, USA) (Fig S1 and S2).

Histological analysis

Formalin-fixed tissue sections (5 μm) were stained with haematoxylin and eosin (POCD; Artarmon, Australia) and histology assessed as described[15]. Total numbers of leukocytes in GVHD target organs were quantified from captured images (Leica DMRB microscope, Wetzlar, Germany) using FIJI is just ImageJ (FIJI) software[45].

Immunohistochemical analysis

To identify human T cells, formalin-fixed tissue sections (5 μm) were deparrifinised, and stained with rabbit anti-hCD3 mAb (clone EP449E) (Abcam, Cambridge, UK) and counterstained with haematoxylin as described[15]. To identify apoptotic cells, an *in-situ*

Apoptosis Detection Kit (Abcam) was used as per the manufacturer's instructions. Immunohistochemistry images were captured using a Leica DMRB microscope. Total numbers of $hCD3^+$ T cell infiltrates in livers and apoptotic cells in liver, skin and small intestine were quantified from captured images using FIJI is just ImageJ (FIJI) software[45].

Cytokine analysis by a flow cytometric multiplex assay

Serum was obtained from mice at end-point as described[15] and cytokine concentrations were measured using a human Th1 LEGENDPlex kit (BioLegend; San Diego, CA, USA) as per the manufacturer's instructions. IFN-γ measurements were reattempted on previously freeze-thawed serum using the Ready-Set-GO! ELISA kit (Thermo Fisher Scientific) as per manufacturer's instructions.

RNA isolation and cDNA synthesis

Tissues removed from euthanized mice were stored in RNAlater (Sigma-Aldrich) at -20°C until required. RNA was isolated using TRIsure reagent (Bioline, London, UK), as per the manufacturer's instructions. Isolated RNA was converted immediately to cDNA using the qScript cDNA Synthesis Kit (Quanta Biosciences, Beverly, MA, USA), as per the manufacturer's instructions, and stored at -20°C. cDNA was checked by polymerase chain reaction (PCR) amplification of the housekeeping gene glyceraldehyde 3-phosphate dehydrogenase (Invitrogen, Carlsbad, CA, USA) for 35 cycles (95°C for 1 min, 55°C for 1 min and 72°C for 1 min) and a holding temperature of 48C. Purity and size of amplicons were confirmed by 2% agarose gel electrophoresis.

Quantitative real-time PCR

Quantitative real-time PCR (qPCR) was performed using TaqMan Universal Master Mix II (Thermo Fisher Scientific, Waltham, MA, USA), according to the manufacturer's instructions, with primers for FAM-labelled human hypoxanthine phosphoribosyl transferase

1 (Hs99999909_m1) and hADORA2A (Hs00948727_g1), and VIC-labelled hP2X7(B) (AIOIXC2) (Thermo Fisher Scientific), as indicated. qPCR cycles consisted of two initial steps of 50°C for 2 min and 95°C for 10 min and 40 cycles of 95°C for 15 s and 60°C for 1 min. qPCR was conducted in triplicate, and were performed on a QuantStudio 5 (Thermo Fisher Scientific), and analysis was conducted using QuantStudio Design and Analysis software version 1.4.1.

ATP-induced YO-PRO-1^{2+} uptake assay

P2X7 pore formation was quantified by measuring ATP-induced YO-PRO-1^{2+} uptake, as described previously[15]. Briefly, freshly isolated hPBMCs in NaCl medium (145 mM NaCl, 5 mM KCl, 5 mM glucose and 10 mM HEPES, pH 7.4) were incubated in the absence or presence of 2 μM APCP[46] or 10 μM BBG[47] (Sigma-Aldrich) for 15 min at 37°C, and then incubated with 1 μM YO-PRO-1 iodide (Molecular Probes, Eugene, OR, USA) in the absence or presence of 1 mM ATP (Sigma-Aldrich) for 5 min. Incubations were stopped by addition of ice-cold NaCl medium containing 20 mM $MgCl_2$ ($MgCl_2$ medium) and centrifugation (300 g for 3 min). Cells were incubated with BV711-conjugated anti-hCD3 mAb for 10 min and washed with NaCl medium. Data were collected using an LSRFortessa X-20 Flow Cytometer (band-pass filter 525/50 for YO-PRO-1^{2+} and 710/50 for BV711) and FACSDiva software version 8.0. The mean fluorescence intensity of YO-PRO-1^{2+} was determined using FlowJo software v8.7.1.

Statistical Analysis

Data are given as mean ± standard error of the mean (SEM). Statistical differences were calculated using Student's *t*-test for single comparisons or one-way analysis of variance (ANOVA) with Tukey's post-hoc test for multiple comparisons. Student's *t*-tests were two-tailed except for immunohistochemistry (one-tailed) where each *a priori* hypothesis was based on intial histology findings. Weight and clinical score were analysed using a repeated

measures two-way ANOVA. Survival (MST) was compared using the log-rank (Mantel-Cox) test. Mortality was compared using Fisher's exact test. All statistical analyses and graphs were generated using GraphPad Prism 5 for PC (GraphPad Software; La Jolla, CA, USA). $P < 0.05$ was considered significant for all tests.

ACKNOWLEDGEMENTS

This project was funded by the Faculty of Science, Medicine and Health, University of Wollongong and Molecular Horizons, University of Wollongong. D.W. was supported by the AMP Tomorrow Fund. We would like to thank Kathryn Friend (BioLegend) for expert advice and assistance with flow cytometric multiplex assays. We would also like to thank Sam Adhikary and Jonathon Williams (University of Wollongong), the technical staff of the Illawarra Health and Medical Research Institute, and the animal house staff at the University of Wollongong rodent facility for assistance.

CONFLICT OF INTEREST

All authors declare that they have no conflicts of interest.

AUTHOR CONTRIBUTIONS

NJG, DW and RS designed the experiments. NJG performed the experiments, analysed the data, prepared the figures and wrote the manuscript. DW and RS supervised the project, reviewed the data and edited the manuscript.

REFERENCES

1. Jagasia M, Arora M, Flowers MED*, et al.* Risk factors for acute GVHD and survival after hematopoietic cell transplantation. *Blood*. 2012; **119**: 296-307.
2. Ferrara JL, Levine JE, Reddy P*, et al.* Graft-versus-host disease. *The Lancet*. 2009; **373**: 1550-1561.
3. Blazar BR, Taylor PA, Panoskaltsis-Mortari A*, et al.* Interleukin-10 dose-dependent regulation of CD4+ and CD8+ T cell- mediated graft-versus-host disease. *Transplantation*. 1998; **66**: 1220-1229.
4. Schneidawind D, Pierini A, Negrin RS. Regulatory T cells and natural killer T cells for modulation of GVHD following allogeneic hematopoietic cell transplantation. *Blood*. 2013; **122**: 3116-3121.
5. Burnstock G. Purine and pyrimidine receptors. *Cell Mol Life Sci*. 2007; **64**: 1471-83.
6. Di Virgilio F, Vuerich M. Purinergic signaling in the immune system. *Auton Neurosci*. 2015; **191**: 117-123.
7. Idzko M, Ferrari D, Eltzschig HK. Nucleotide signalling during inflammation. *Nature*. 2014; **509**: 310.
8. D'Addio F, Vergani A, Potena L*, et al.* P2X7R mutation disrupts the NLRP3-mediated Th program and predicts poor cardiac allograft outcomes. *J Clin Invest*. 2018; **128:** 3490-3503.
9. Ledderose C, Liu K, Kondo Y*, et al.* Purinergic P2X4 receptors and mitochondrial ATP production regulate T cell migration. *J Clin Invest*. 2018; **128**: 3583-3594.
10. Antonioli L, Pacher P, Vizi ES*, et al.* CD39 and CD73 in immunity and inflammation. *Trend Mol Med*. 2013; **19**: 355-367.
11. Castillo-Leon E, Dellepiane S, Fiorina P. ATP and T-cell-mediated rejection. *Curr Opin Org Transpl*. 2018; **23**: 34-43.
12. Wilhelm K, Ganesan J, Müller T*, et al.* Graft-versus-host disease is enhanced by extracellular ATP activating P2X7R. *Nat Med*. 2010; **16**: 1434-1438.
13. Fowler BJ, Gelfand BD, Kim Y*, et al.* Nucleoside reverse transcriptase inhibitors possess intrinsic anti-inflammatory activity. *Science*. 2014; **346**: 1000-3.
14. Zhong X, Zhu F, Qiao J*, et al.* The impact of P2X7 receptor antagonist, brilliant blue G on graft-versus-host disease in mice after allogeneic hematopoietic stem cell transplantation. *Cell Immunol*. 2016; **310**: 71-77.
15. Geraghty NJ, Belfiore L, Ly D*, et al.* The P2X7 receptor antagonist Brilliant Blue G reduces serum human interferon-γ in a humanized mouse model of graft-versus-host disease. *Clin Exp Immunol*. 2017; **190**: 79-95.
16. Geraghty NJ, Watson D, Sluyter R. Long-term treatment with the P2X7 receptor antagonist Brilliant Blue G reduces liver inflammation in a humanized mouse model of graft-versus-host disease. *Cell Immunol*. 2019; **336**: 12-19.
17. Klambt V, Wohlfeil SA, Schwab L*, et al.* A Novel Function for P2Y2 in Myeloid Recipient-Derived Cells during Graft-versus-Host Disease. *J Immunol*. 2015; **195**: 5795-5804.
18. Lappas CM, Liu P-C, Linden J*, et al.* Adenosine A2A receptor activation limits graft-versus-host disease after allogenic hematopoietic stem cell transplantation. *J Leuk Biol*. 2010; **87**: 345-354.
19. Han KL, Thomas SV, Koontz SM*, et al.* Adenosine A2A Receptor Agonist–Mediated Increase in Donor-Derived Regulatory T Cells Suppresses Development of Graft-versus-Host Disease. *J Immunol*. 2013; **190**: 458-468.

20. Tsukamoto H, Chernogorova P, Ayata K*, et al.* Deficiency of CD73/ecto-5′-nucleotidase in mice enhances acute graft-versus-host disease. *Blood*. 2012; **119**: 4554-4564.
21. Wang L, Fan J, Chen S*, et al.* Graft-versus-Host Disease Is Enhanced by Selective CD73 Blockade in Mice. *PLoS ONE*. 2013; **8**: e58397.
22. Moody CJ, Meghji P, Burnstock G. Stimulation of P1-purinoceptors by ATP depends partly on its conversion to AMP and adenosine and partly on direct action. *Eur J Pharmacol*. 1984; **97**: 47-54.
23. Covarrubias R, Chepurko E, Reynolds A*, et al.* Role of the CD39/CD73 Purinergic Pathway in Modulating Arterial Thrombosis in Mice. *Arter Thromb Vasc Biol*. 2016; **36**: 1809-1820.
24. Geraghty NJ, Belfiore L, Adhikary SR*, et al.* Increased splenic human $CD4^+$:$CD8^+$ T cell ratios, serum human interferon-γ and intestinal human interleukin-17 are associated with clinical graft-versus-host disease in humanized mice. *Transplant Immunol*. 2019.
25. Glucksberg H, Storb R, Fefer A*, et al.* Clinical manifestations of graft-versus-host disease in human recipients of marrow from HL-A-matched sibling donors. *Transplantation*. 1974; **18**: 295-304.
26. Schroeder MA, DiPersio JF. Mouse models of graft-versus-host disease: Advances and limitations. *Dis Model Mech*. 2011; **4**: 318-333.
27. King M, Covassin L, Brehm M*, et al.* Human peripheral blood leucocyte non-obese diabetic-severe combined immunodeficiency interleukin-2 receptor gamma chain gene mouse model of xenogeneic graft-versus-host-like disease and the role of host major histocompatibility complex. *Clin Exp Immunol*. 2009; **157**: 104-118.
28. El Yacoubi M, Ledent C, Parmentier M*, et al.* SCH 58261 and ZM 241385 differentially prevent the motor effects of CGS 21680 in mice: evidence for a functional 'atypical' adenosine A2A receptor. *Eur J Pharmacol*. 2000; **401**: 63-77.
29. Abo-Salem OM, Hayallah AM, Bilkei-Gorzo A*, et al.* Antinociceptive Effects of Novel A_{2B} Adenosine Receptor Antagonists. *J Pharmacol Exp Ther*. 2004; **308**: 358-366.
30. Shultz LD, Lyons BL, Burzenski LM*, et al.* Human lymphoid and myeloid cell development in NOD/LtSz-scid IL2Rγnull mice engrafted with mobilized human hemopoietic stem cells. *J Immunol*. 2005; **174**: 6477-6489.
31. King MA, Covassin L, Brehm MA*, et al.* Human peripheral blood leucocyte non-obese diabetic-severe combined immunodeficiency interleukin-2 receptor gamma chain gene mouse model of xenogeneic graft-versus-host-like disease and the role of host major histocompatibility complex. *Clin Exp Immunol*. 2009; **157**: 104-118.
32. Brehm MA, Kenney LL, Wiles MV*, et al.* Lack of acute xenogeneic graft- versus-host disease, but retention of T-cell function following engraftment of human peripheral blood mononuclear cells in NSG mice deficient in MHC class I and II expression. *FASEB J*. 2018; fj201800636R.
33. Kawasaki Y, Sato K, Hayakawa H*, et al.* Comprehensive Analysis of the Activation and Proliferation Kinetics and Effector Functions of Human Lymphocytes, and Antigen Presentation Capacity of Antigen-Presenting Cells in Xenogeneic Graft-Versus-Host Disease. *Biol Blood Marrow Transplant*. 2018; **24**: 1563-74.
34. Abraham S, Guo H, Choi JG*, et al.* Combination of IL-10 and IL-2 induces oligoclonal human CD4 T cell expansion during xenogeneic and allogeneic GVHD in humanized mice. *Heliyon*. 2017; **3**: e00276.

35. Pérol L, Martin GH, Maury S*, et al.* Potential limitations of IL-2 administration for the treatment of experimental acute graft-versus-host disease. *Immunol Lett*. 2014; **162**: 173-184.
36. Zeng D, Lewis D, Dejbakhsh-Jones S*, et al.* Bone Marrow NK1.1$^-$ and NK1.1$^+$ T Cells Reciprocally Regulate Acute Graft versus Host Disease. *J Exp Med*. 1999; **189**: 1073-1081.
37. Kim JH, Choi EY, Chung DH. Donor Bone Marrow Type II (Non-Vα14Jα18 CD1d-Restricted) NKT Cells Suppress Graft-Versus-Host Disease by Producing IFN-γ and IL-4. *J Immunol*. 2007; **179**: 6579-6587.
38. Schneidawind D, Baker J, Pierini A*, et al.* Third-party CD4+ invariant natural killer T cells protect from murine GVHD lethality. *Blood*. 2015; **125**: 3491-500.
39. Audigé A, Rochat MA, Li D*, et al.* Long-term leukocyte reconstitution in NSG mice transplanted with human cord blood hematopoietic stem and progenitor cells. *BMC Immunol*. 2017; **18**: 28.
40. Palamides P, Jodeleit H, Föhlinger M*, et al.* A mouse model for ulcerative colitis based on NOD-*scid* IL2R γ^{null} mice reconstituted with peripheral blood mononuclear cells from affected individuals. *Dis Model Mech*. 2016; **9**: 985-997.
41. Jodeleit H, Palamides P, Beigel F*, et al.* Design and validation of a disease network of inflammatory processes in the NSG-UC mouse model. *J Transl Med*. 2017; **15**: 265.
42. Seldon TA, Pryor R, Palkova A*, et al.* Immunosuppressive human anti-CD83 monoclonal antibody depletion of activated dendritic cells in transplantation. *Leukemia*. 2015; **30**: 692.
43. Shlomchik WD, Couzens MS, Tang CB*, et al.* Prevention of graft versus host disease by inactivation of host antigen- presenting cells. *Science*. 1999; **285**: 412-415.
44. Markey KA, Banovic T, Kuns RD*, et al.* Conventional dendritic cells are the critical donor APC presenting alloantigen after experimental bone marrow transplantation. *Blood*. 2009; **113**: 5644-5649.
45. Schindelin J, Arganda-Carreras I, Frise E*, et al.* Fiji: an open-source platform for biological-image analysis. *Nat Meth*. 2012; **9**: 676-682.
46. Zhou X, Zhi X, Zhou P*, et al.* Effects of ecto-5′-nucleotidase on human breast cancer cell growth in vitro and in vivo. *Oncol Rep*. 2007; **17**: 1341-1346.
47. Jiang L-H, Mackenzie AB, North RA*, et al.* Brilliant blue G selectively blocks ATP-gated rat P2X7 receptors. *Mol Pharmacol*. 2000; **58**: 82-88.

FIGURE LEGENDS

Figure 1. APCP reduces human CD4$^+$CD39$^-$CD73$^-$ cells but not other T cell subsets in a humanised mouse model of GVHD

(**a-m**) The percentage of human leukocytes in (**a-c**) blood at 3 weeks post-hPBMC injection and (**d-m**) spleens at end-point from humanised NSG mice injected with saline (control) or the CD39/CD73 inhibitor APCP (50 mg/kg) were determined by flow cytometry. (**a, d**) hCD45$^+$ leukocytes are expressed as a percentage of total (mCD45$^+$ and hCD45$^+$) leukocytes. (**b, e**) T cells (hCD3$^+$hCD19$^-$) and (**c, k**) non-B/T cells (hCD3$^-$hCD19$^-$) are expressed as a

percentage of $hCD45^+$ leukocytes. (**f**) $hCD4^+$ and $hCD8^+$ T cell subsets are expressed as a percentage of $hCD3^+$ leukocytes. ** $P < 0.005$, *** $P < 0.0001$ compared to $hCD8^+$ T cells. (**g-h**) The expression of hCD39 and hCD73 was analysed on (**g**) $hCD4^+$ and (**h**) $hCD8^+$ T cell subsets. * $P < 0.05$ compared to respective saline control. (**i**) iNKT cells ($hV\alpha24\text{-}J\alpha18^+$) are expressed as a percentage of $hCD3^+hCD19^-$ T cells and (**j**) Treg cells ($hCD25^+hCD127^{lo}$) are expressed as a percentage of $hCD3^+hCD4^+$ T cells. (**l**) monocytes ($hCD14^+CD83^-$) and (**m**) DCs ($hCD14^-CD83^+$) are expressed as a percentage of non-B/T cells. (**a-m**) Data represents group means ± SEM; symbols represent individual mice (saline $n = 9$, APCP $n = 8$-9) from two independent experiments.

Figure 2. CD73 blockade worsens weight loss in a humanised mouse model of GVHD

(**a-c**) Humanised NSG mice injected with saline (control) or the CD39/CD73 inhibitor APCP (50 mg/kg) were monitored for (**a**) weight loss, (**b**) clinical score and (**c**) survival over 10 weeks. * $P < 0.05$ compared to saline-injected mice. Data represents (**a-b**) group means ± SEM or (**c**) percent survival (saline $n = 9$, APCP $n = 9$) from two independent experiments.

Figure 3. CD73 blockade augments liver histology in a humanised mouse model of GVHD

(**a-f**) Liver, small intestine and skin, collected at end-point, were sectioned and stained with (**a**) haematoxylin and eosin, (**c**) anti-hCD3 monoclonal antibody with DAB detection system and haematoxylin or (**e**) TUNEL with DAB detection system and methyl green. Images were captured by microscopy, and (**b**) leukocyte and (**d**) human T cell infiltration, and (**f**) apoptosis quantified using FIJI. Each image is representative of eight mice per group for histology, or four mice per goup for IHC from two independent experiments; (**a, c, e**) bar represents 100 μm. * $P < 0.05$ compared to respective saline control. (**b, f**) data represents group means ± SEM; symbols represent individual mice; * $P < 0.05$ compared to respective saline control.

Figure 4. CD73 blockade increases serum hIL-2 concentrations but does not affect A_{2A} or P2X7 expression in a humanised mouse model of GVHD

(**a-d**) Serum was collected at end-point. Concentrations of serum human (**a**) IL-2, (**b**) IL-6, (**c**) IL-10 and (**d**) TNF-α were analysed using a flow cytometric multiplex assay. * $P < 0.05$ compared to respective saline control. Data represents group means ± SEM (saline $n = 8$, APCP $n = 9$) from two independent experiments. (**e-f**) Spleens were collected at end-point. The relative expression of (**e**) hA_{2A} and (**f**) hP2X7 were examined by qPCR. Data represent group mean ± SEM; symbols represent individual mice (saline $n = 7$, APCP $n = 7$) from two independent experiments. (**g**) Freshly isolated hPBMCs were pre-incubated for 15 min in the absence or presence of 2 μM APCP or 10 μM BBG and then with 1 μM YO-PRO-1^{2+} in the absence or presence of 1 mM ATP for 5 min at 37 °C. Assays were stopped by addition of $MgCl_2$ medium and centrifugation. Cells were then labelled with BV711-conjugated hCD3 mAb. YO-PRO-1^{2+} uptake into $hCD3^+$ T cells was assessed by flow cytometry. ** $P < 0.005$ compared to control. Data represents group means ± SEM ($n = 3$ donors) from one experiment.

Figure 5. Caffeine does not impact human leukocyte engraftment in a humanised mouse model of GVHD

(**a-m**) The percentage of human leukocytes in (**a-c**) blood at 3 weeks post-hPBMC injection and (**d-m**) spleens at end-point from humanised NSG mice injected with saline (control) or the AR antagonist caffeine (10 mg/kg) were determined by flow cytometry. (**a, d**) $hCD45^+$ leukocytes are expressed as a percentage of total ($mCD45^+$ and $hCD45^+$) leukocytes. (**b, e**) T cells ($hCD3^+hCD19^-$) and (**c, k**) non-B/T cells ($hCD3^-hCD19^-$) are expressed as a percentage of $hCD45^+$ leukocytes. (**f**) $hCD4^+$ and $hCD8^+$ T cell subsets are expressed as a percentage of $hCD3^+$ leukocytes. *** $P < 0.0001$ compared to $hCD8^+$ T cells. (**g, h**) The expression of hCD39 and hCD73 was analysed on (**g**) $hCD4^+$ and (**h**) $hCD8^+$ T cell subsets. **i** iNKT cells ($hV\alpha24\text{-}J\alpha18^+$) are expressed as a percentage of $hCD3^+hCD19^-$ T cells and (**j**) Treg cells

($hCD25^+hCD127^{lo}$) are expressed as a percentage of $hCD3^+$ $hCD4^+$ T cells. (**l**) monocytes ($hCD14^+CD83^-$) and (**m**) DCs ($hCD14^-CD83^+$) are expressed as a percentage of non-B/T cells. (**a-m**) Data represents group means ± SEM; symbols represent individual mice (saline *n* = 15, caffeine *n* = 13) from three independent experiments.

Figure 6. Caffeine does not impact disease in a humanised mouse model of GVHD

(**a-h**) Humanised NSG mice injected with saline (control) or the AR antagonist caffeine (10 mg/kg) were monitored for (**a**) weight loss, (**b**) clinical score, and (**c**) survival over 10 weeks. Data represents (**a-b**) group means ± SEM or (**c**) percent survival (saline *n* = 9, caffeine *n* = 9). (**d-h**) Tissues and serum were collected at end-point. (**d**) Liver, small intestine and skin were sectioned and stained with haematoxylin and eosin and images were captured by microscopy, with each image representative of 13 mice per group; bar represents 100 μm. (**e-h**) Concentrations of serum human (**e**) IL-2, (**f**) IL-6, (**g**) IL-10 and (**h**) TNF-α were analysed using a flow cytometric multiplex assay. Data represents group means ± SEM (saline *n* = 15, caffeine *n* = 13) from three independent experiments.

SUPPLEMENTARY FIGURES

Fig. S1. Flow cytometric gating of leukocytes in blood from humanised mice

The percentage of human leukocytes in blood at 3 weeks post-hPBMC injection collected from all humanised NSG mice were determined by flow cytometry. Forward scatter area (FSC-A) and forward scatter height (FSC-H) were used to identify single cells (far left panel). Forward scatter (FSC-A) and side scatter (SSC-A) (middle left panel) were used to identify and subsequently analyse the percentages of human leukocytes ($hCD45^+mCD45^-$; middle right panel), which comprised T and non-B/T cells ($hCD3^+hCD19^-$ and $hCD3^-hCD19^-$ respectively; far right panel).

Fig. S2. Flow cytometric gating of leukocytes in spleens from humanised mice

(**a-b**) The percentage of human leukocytes in spleens at end-point collected from all humanised NSG mice were determined by flow cytometry. (**a)** Forward scatter (FSC-A, FSC-H) and side scatter (SSC-A) were used to identify and subsequently analyse single leukocytes (top left and middle panels). These leukocytes were analysed to determine the percentages of human leukocytes ($hCD45^+mCD45^-$; top right panel), and subsequently used to identify T cells ($hCD3^+hCD19^-$; bottom left panel) and iNKT cells ($hCD3^+hCD19^-hV\alpha24\text{-}J\alpha18^+$; bottom middle panel), or non-B/T cells ($hCD3^-hCD19^-$; bottom left panel), which were subsequently used to identify monocytes and DCs ($hCD14^+CD83^-$ and $hCD14^-CD83^+$ respectively; bottom right panel). (**b**) Single leukocytes were gated as above. T cells were identified ($hCD3^+$; top left panel), and subsequently used to determine $hCD4^+$ and $hCD8^+$ T cell subsets (top middle panel), and hCD39 and hCD73 expression on $hCD4^+$ (top right panel) and $hCD8^+$ (bottom left panel) T cells was analysed. $hCD4^+$ T cells were also gated to identify Tregs ($hCD25^+hCD127^{lo}$; bottom right panel).

Fig. S3. Flow cytometric gating for ATP-induced YO-PRO-1^{2+} uptake into human T cells

ATP-induced YO-PRO-1^{2+} uptake into freshly isolated hPBMCs was determined by flow cytometry. Forward scatter (FSC-A, FSC-H) and side scatter (SSC-A) were used to identify and subsequently analyse single leukocytes (left and middle panels). BV711-conjugated hCD3 was then used to identify and analyse T cells (right panel).

TABLE

Table 1. Clinical scoring of GVHD in humanised NSG mice.

GRADE	0	1	2
Weight loss	< 5%	5% to 10%	> 10%
Posture	Normal	Hunching noted only at rest	Severe hunching
Activity	Normal	Mild to moderately decreased	Stationary unless stimulated
Fur texture	Normal	Mild to moderate ruffling	Severe ruffling poor grooming
Skin Integrity	Normal	Scaling of paws/tail	Obvious areas of involved skin

Mice with a total score of 8 or more were euthanized that same day.

Table 2. APCP reduces human $CD4^+CD39^-CD73^-$ T cells in a humanised mouse model of GVHD.

T cell subset	hCD39 and hCD73 Expression	Saline	APCP	*P*-value
$hCD4^+$	$CD39^+CD73^-$	5.5 ± 2.1%	10.2 ± 4.1%	0.3441
	$CD39^-CD73^+$	3.7 ± 0.9%	13.1 ± 5.5%	0.1347
	$CD39^+CD73^+$	0.8 ± 0.4%	1.3 ± 0.4%	0.4247
	$CD39^-CD73^-$	89.9 ± 2.4%	75.4 ± 5.8%	0.0441*
$hCD8^+$	$CD39^+CD73^-$	36.4 ± 5.0%	41.4 ± 3.0%	0.3867
	$CD39^-CD73^+$	2.8 ± 0.6%	3.8 ± 1.0%	0.4342
	$CD39^+CD73^+$	4.1 ± 1.2%	5.5 ± 1.6%	0.5035
	$CD39^-CD73^-$	56.7 ± 5.8%	49.3 ± 4.6%	0.3247

All data obtained from Figure 1g-h. * $P < 0.05$ compared to respective saline control.

Table 3. Caffeine does not impact human $CD39^{+/-}CD73^{+/-}$ T cells in a humanised mouse model of GVHD.

T cell subset	hCD39 and hCD73 Expression	Saline	Caffeine	*P*-value
$hCD4^+$	$CD39^+CD73^-$	11.0 ± 3.6%	14.2 ± 4.6%	0.5926
	$CD39^-CD73^+$	5.3 ± 1.9%	3.2 ± 1.0%	0.3572
	$CD39^+CD73^+$	0.7 ± 0.3%	0.8 ± 0.2%	0.9430
	$CD39^-CD73^-$	83.0 ± 3.5%	81.8 ± 4.4%	0.8425
$hCD8^+$	$CD39^+CD73^-$	39.5 ± 5.4%	33.3 ± 6.2%	0.4544
	$CD39^-CD73^+$	5.9 ± 2.8%	3.3 ± 0.7%	0.3922
	$CD39^+CD73^+$	5.2 ± 2.0%	4.9 ± 1.4%	0.9055
	$CD39^-CD73^-$	50.6 ± 6.0%	57.4 ± 6.9%	0.4627

All data obtained from Figure 5g-h.

SUPPLEMENTARY TABLE

Table S1. Monoclonal antibodies used for flow cytometry.

Target	Fluorochrome	Clone*
CD14	BV421	MϕP9
CD127	BV421	HIL-7R-M21
CD3	BV711	UCHT1
CD45	FITC	HI30
CD8	FITC	RPA-T8
CD25	PE	M-A251
CD3	PE	UCHT1
CD83	PE	HB15e
CD4	PerCP-Cy5.5	L200
CD45	PerCP-Cy5.5	30-F11
CD73	PE-Cy7	AD2
Vα24-Jα14	PE-Cy7	6B11
CD19	APC	HIB19
CD39	APC	TU66

*All antibodes mouse anti-human except clone 30-F11 (rat anti-mouse); all antibodies from BD Biosciences except clone 6B11 (BioLegend).

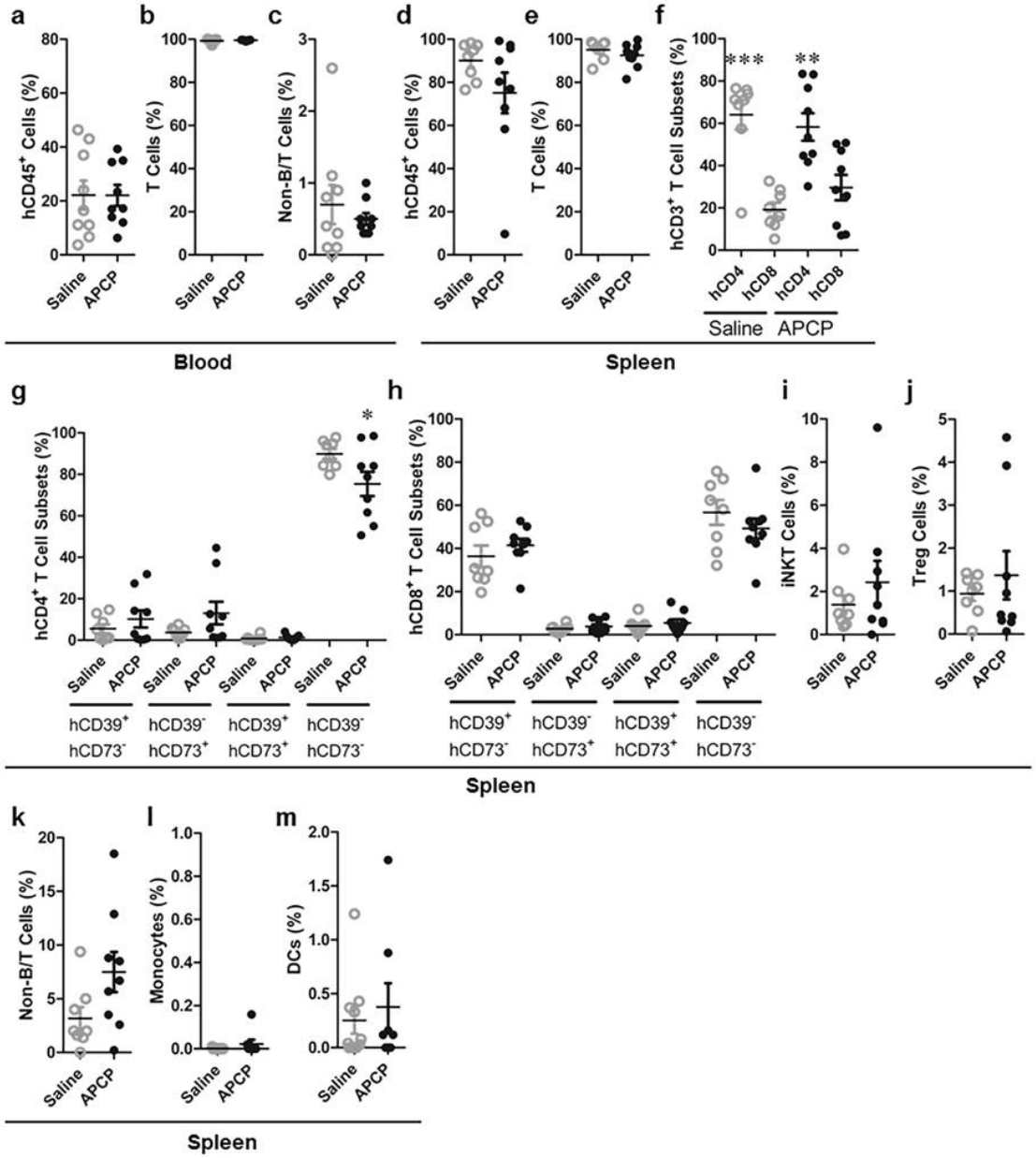
a
b
c
d
e
f
hCD45+ Cells (%)
T Cells (%)
Non-B/T Cells (%)
hCD45+ Cells (%)
T Cells (%)
hCD3+ T Cell Subsets (%)
***
**
Saline
APCP
hCD4
hCD8
Blood
Spleen
g
h
i
j
hCD4+ T Cell Subsets (%)
hCD8+ T Cell Subsets (%)
iNKT Cells (%)
Treg Cells (%)
*
hCD39+ hCD73-
hCD39- hCD73+
hCD39+ hCD73+
hCD39- hCD73-
Spleen
k
l
m
Non-B/T Cells (%)
Monocytes (%)
DCs (%)
Spleen

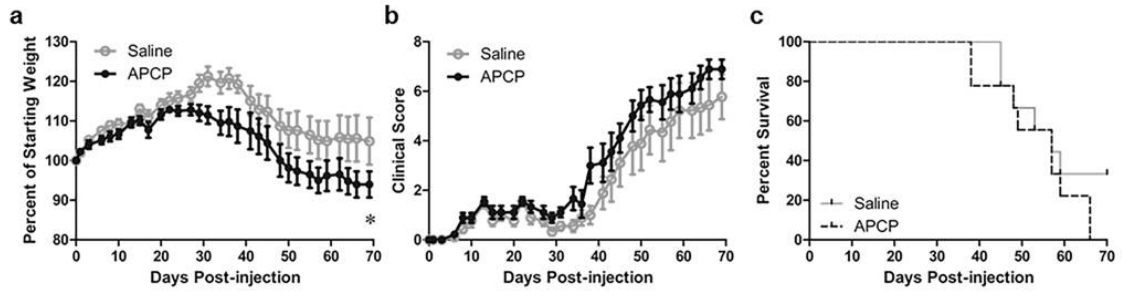
a
Percent of Starting Weight
Saline
APCP
*
Days Post-injection
b
Clinical Score
Saline
APCP
Days Post-injection
c
Percent Survival
Saline
APCP
Days Post-injection

704

705

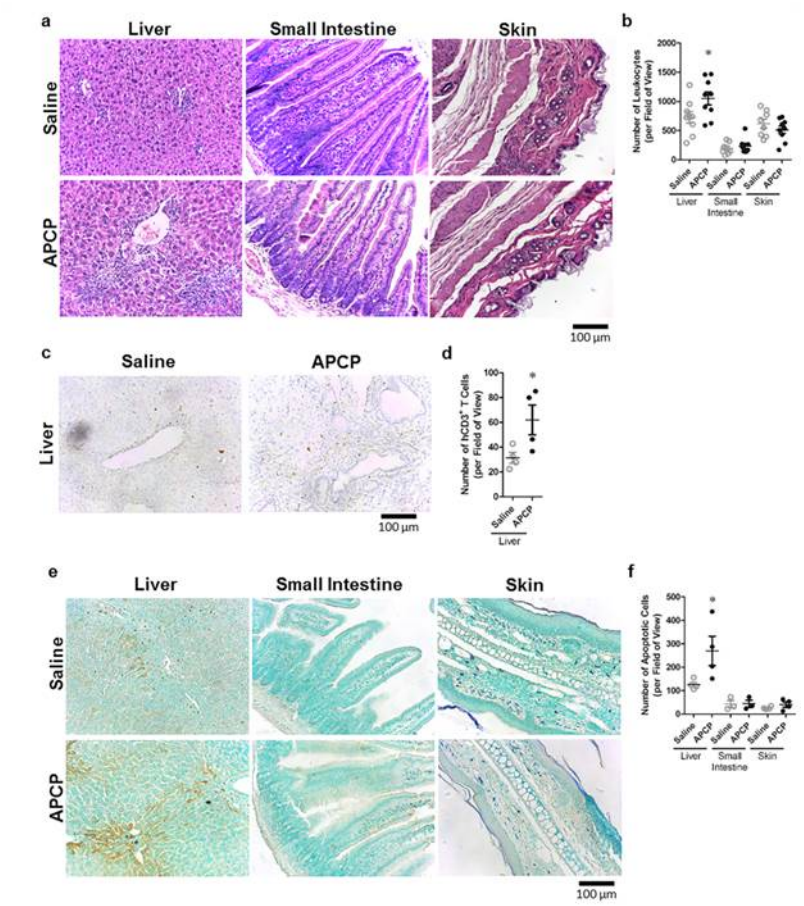
a
Liver
Small Intestine
Skin
Saline
APCP
100 µm
b
Number of Leukocytes (per Field of View)
Saline
APCP
Liver
Small Intestine
Skin
c
Saline
APCP
Liver
100 µm
d
Number of hCD3+ T Cells (per Field of View)
Saline
APCP
Liver
e
Liver
Small Intestine
Skin
Saline
APCP
100 µm
f
Number of Apoptotic Cells (per Field of View)
Saline
APCP
Liver
Small Intestine
Skin

706

707

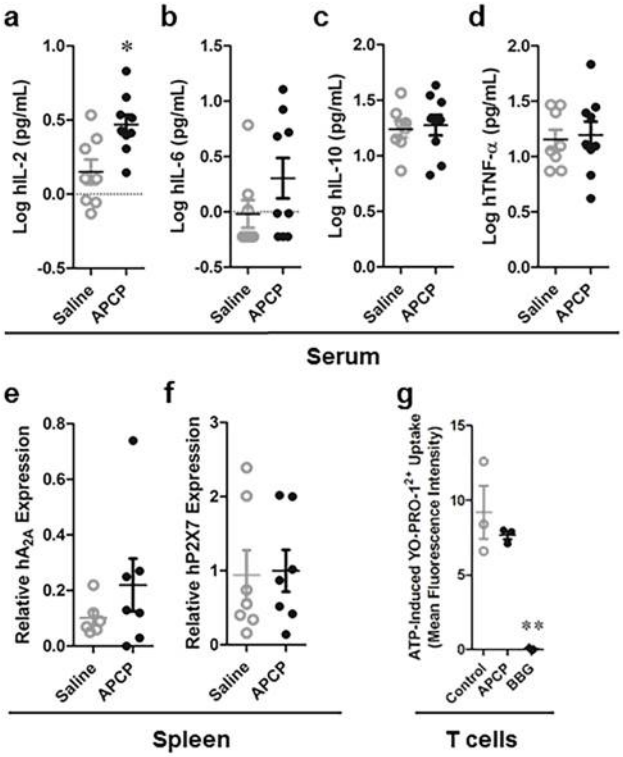
a
b
c
d
Log hIL-2 (pg/mL)
Log hIL-6 (pg/mL)
Log hIL-10 (pg/mL)
Log hTNF-α (pg/mL)
Saline
APCP
Serum
e
f
g
Relative hA2A Expression
Relative hP2X7 Expression
ATP-Induced YO-PRO-1 2+ Uptake (Mean Fluorescence Intensity)
Control
APCP
BBG
Spleen
T cells

708

709

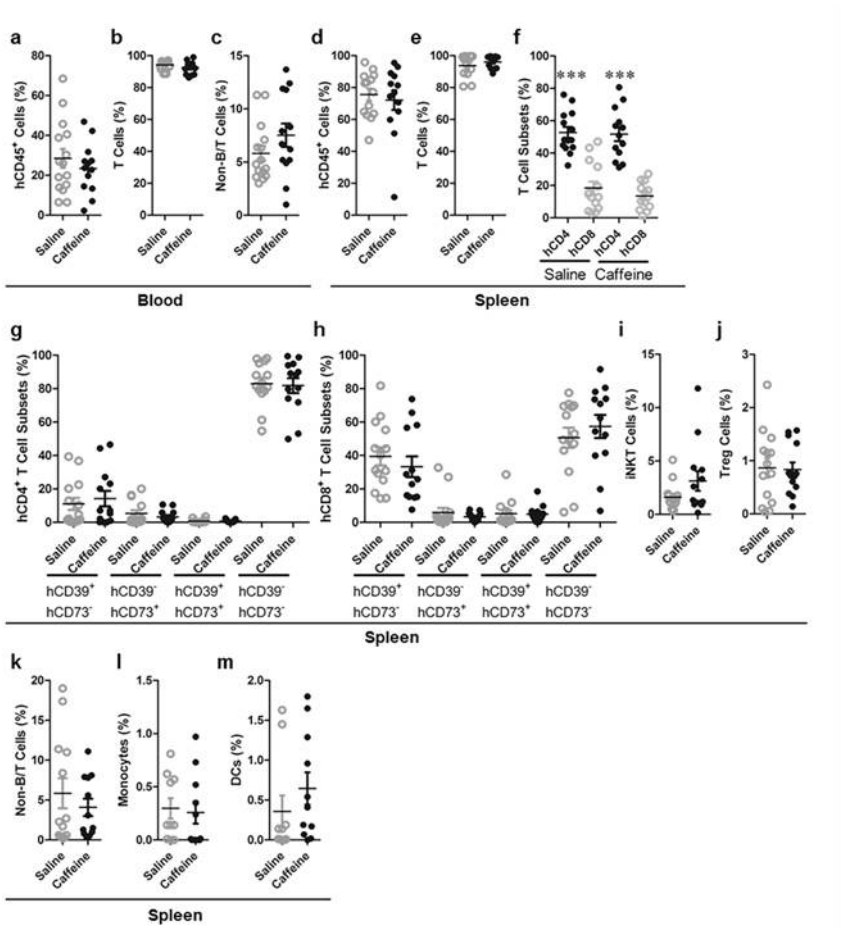
a
b
c
d
e
f
hCD45+ Cells (%)
T Cells (%)
Non-B/T Cells (%)
hCD45+ Cells (%)
T Cells (%)
T Cell Subsets (%)
***
***
Saline
Caffeine
hCD4
hCD8
hCD4
hCD8
Saline Caffeine
Blood
Spleen
g
h
i
j
hCD4+ T Cell Subsets (%)
hCD8+ T Cell Subsets (%)
iNKT Cells (%)
Treg Cells (%)
hCD39+ hCD73-
hCD39- hCD73+
hCD39+ hCD73+
hCD39- hCD73-
Spleen
k
l
m
Non-B/T Cells (%)
Monocytes (%)
DCs (%)
Spleen

710

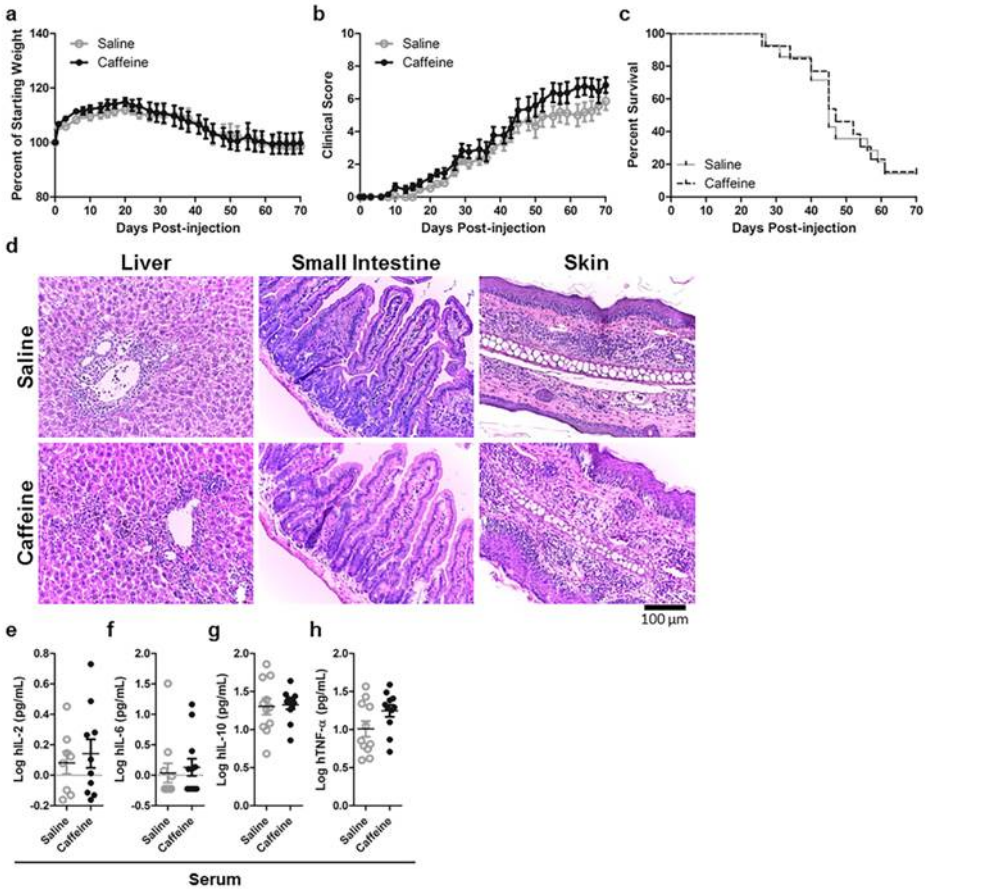
a
Percent of Starting Weight
Saline
Caffeine
Days Post-injection
b
Clinical Score
Saline
Caffeine
Days Post-injection
c
Percent Survival
Saline
Caffeine
Days Post-injection
d
Liver
Small Intestine
Skin
Saline
Caffeine
100 µm
e
Log hIL-2 (pg/mL)
f
Log hIL-6 (pg/mL)
g
Log hIL-10 (pg/mL)
h
Log hTNF-α (pg/mL)
Saline
Caffeine
Serum

711

712

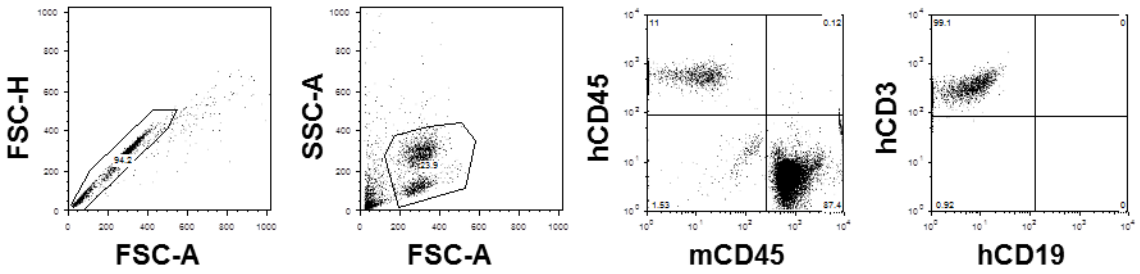
FSC-H
FSC-A
94.2
SSC-A
FSC-A
hCD45
mCD45
11
0.12
1.53
87.4
hCD3
hCD19
99.1
0
0.92
0

713

714

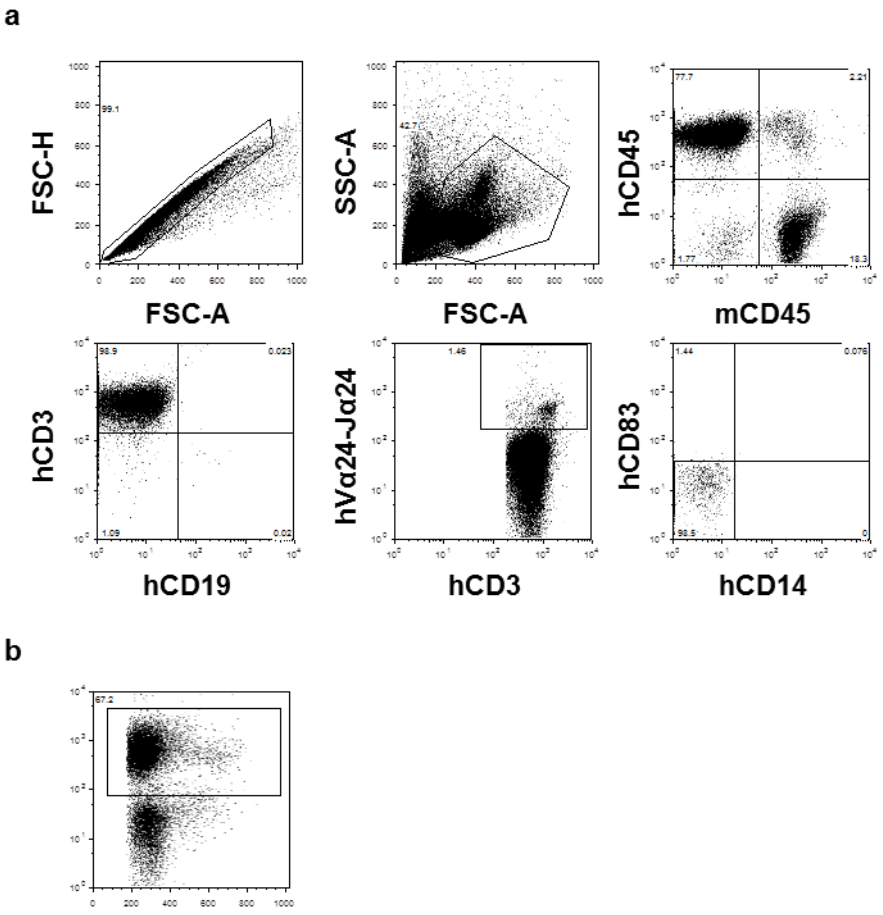
a
FSC-H
FSC-A
99.1
SSC-A
FSC-A
42.7
hCD45
mCD45
77.7
2.21
1.77
18.3
hCD3
hCD19
98.9
0.023
1.09
0.02
hVα24-Jα24
hCD3
1.46
hCD83
hCD14
1.44
0.076
98.5
0
b
87.2

715

716

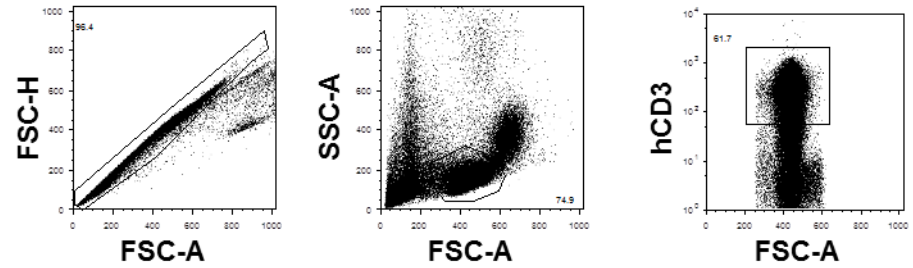

717